



# Magnetic field map of the Wilhelm Archipelago shelf zone, West Antarctica

Volodymyr Bakhmutov<sup>1,2</sup> · Tamara Yegorova<sup>1,3</sup> · Mariya Bakarzhiyeva<sup>1</sup> · Olexandr Mytrokhyn<sup>4</sup> · Viktor Shpyra<sup>1</sup> · Mykhailo Orlyuk<sup>1</sup> · Valentyn Maksymchuk<sup>5</sup> · Viktor Tarasov<sup>1</sup> · Andrii Romenets<sup>1</sup> · Yevheniy Nakalov<sup>5</sup> · Yevhenii Brillinh<sup>5</sup> · Oleh Romanyuk<sup>5</sup> · Yurii Otruba<sup>6</sup> · Dmytro Litvinov<sup>7</sup>

Received: 24 November 2022 / Accepted: 12 September 2023 / Published online: 11 October 2023  
© The Author(s) 2023

## Abstract

The Antarctic Digital Magnetic Anomaly Project is an international research effort to construct a magnetic map of the continent based on ground, satellite, marine, and aeromagnetic surveys. This paper reports the magnetic mapping of the shelf zone in the SE part of the Wilhelm Archipelago, West Antarctica, based on magnetic surveys conducted with Zodiac boats. A spectacular feature of this area is the strong magnetic anomaly of the Antarctic Peninsula (AP) batholith, which was the product of subduction-related Mesozoic–Cenozoic arc magmatism on the former margin of Western Gondwana. We constructed and analyzed a detailed magnetic map of magnetic field anomalies using field observations of rock exposures on the islands and magnetic properties of rocks from laboratory data. The oldest volcanic rocks of Jurassic to Lower Cretaceous age relate to N-NE trending bands of negative magnetic field. The largest feature in the study area is an Upper Cretaceous/Paleogene granodiorite complex that produces a positive magnetic anomaly. Many smaller anomalies are also present over gabbroid bodies of Cretaceous age. Two-dimensional magnetic modeling shows that heterogeneities in the upper crust may have magnetic susceptibilities in the range of 0.005–0.13 SI. Magnetic field anomalies also delineate an orthogonal system of tectonic faults, including the main NE fault along the Penola Strait (sub-parallel to the AP coastline) and four intersecting faults. These fault systems may be associated with different stages of continental margin evolution along the Antarctic Peninsula.

**Keywords** Antarctic Peninsula · Wilhelm Archipelago · Geophysical survey · Magnetic anomalies · Crustal studies

---

Edited by Prof. Bogdan Mihai Niculescu (ASSOCIATE EDITOR) / Prof. Gabriela Fernández Viejo (CO-EDITOR-IN-CHIEF).

---

✉ Volodymyr Bakhmutov  
bakhmutovvg@gmail.com

<sup>1</sup> Subbotin Institute of Geophysics, National Academy of Sciences of Ukraine, 32 Palladina Av., Kyiv 03680, Ukraine

<sup>2</sup> Institute of Geophysics Polish Academy of Sciences, 64 Księcia Janusza, 01-452 Warszawa, Poland

<sup>3</sup> Department of Life Sciences and Environmental Sustainability, University of Parma, Parco Area delle Scienze 11/A, Campus, I-43124 Parma, Italy

<sup>4</sup> Educational-Scientific Institute 'Institute of Geology', Taras Shevchenko National University of Kyiv, 90 Vasylykivska Str., Kyiv 03022, Ukraine

<sup>5</sup> Carpathian Branch of Subbotin Institute of Geophysics, National Academy of Sciences of Ukraine, 3-B Naukova Str., Lviv 79060, Ukraine

<sup>6</sup> State Institution National Antarctic Scientific Center, Ministry of Education and Science of Ukraine, 16 Taras Shevchenko Blvd, Kyiv 01601, Ukraine

<sup>7</sup> Institute of Geological Sciences, National Academy of Sciences of Ukraine, 55-b O. Honchar Str., Kyiv 01054, Ukraine

## Introduction

Over the past 15–20 years, a unified database for the Antarctic continent and surrounding seas has been in development under the Antarctic Digital Magnetic Anomaly Project (ADMAP; Golynsky et al. 2001, 2013). The existing magnetic database has been supplemented by the results of satellite measurements (5.8 million line-km) from the Magsat, Ørsted, and CHAMP missions, which allowed the construction of a new magnetic map of Antarctica (Kim et al. 2004, 2007). In the last decade, the ADMAP database has been significantly supplemented by new marine and aeromagnetic surveys, as well as by previously unpublished surveys. The bulk of the new data (around 500,000 line-km) is from East Antarctica. In addition, new data from regions of Antarctica, as well as from the continental margin of the Antarctic Peninsula and the Ross Sea, was included in a new map of magnetic field anomalies in East Antarctica (Golynsky et al. 2013), and more complete version of ADMAP-1 (von Frese et al. 2002; Ferraccioli et al. 2013) was prepared.

The second generation Antarctic magnetic anomaly compilation (the ADMAP-2) contains more than 3.5 million line-km of airborne and shipborne data and provides the most complete dataset of magnetic properties of the Antarctic crust (Golynsky et al. 2018). The map reveals a wide variety of magnetic anomalies in crustal terranes of differing lithology, age, geothermal activity and tectonic affinity.

The magnetic surveys, conducted in different parts of Antarctica by various countries and organizations, contribute strongly to the study of the magnetic field of the continent and provide new constraints on composition and tectonic processes in the crust. Our study area belongs to the Antarctic Peninsula (AP), mainly its shelf zone. That is the magmatic arc formed in Mesozoic–Cenozoic at the Gondwana margin, which is characterized by extensive magnetic and gravity anomalies (Fig. 1A) and is the best studied region in Antarctica by deep marine seismic studies (Środa et al. 1997; Janik 1997; Yegorova et al. 2011).

This paper represents the results of magnetic surveys conducted during several field seasons in the area of Ukrainian Antarctic Station (UAS) with the objective of constructing the magnetic anomaly map. The new magnetic survey on the AP could reveal great diversity of the rocks composing the magmatic arc of the AP—volcanic and plutonic ones including mafic and ultramafic rocks that are rich in ore mineralization. Since the composition of rocks is known only where ice-free outcrops exist on islands and the AP coast, the map of the magnetic field anomalies is essential for tracing the areal distribution, size, and interrelations of magmatic bodies.

Thus, the objective of our work is to build a magnetic map of the area of the UAS, and its geological and tectonic

interpretation carried out by taking into account new data from field geological and structural studies, and laboratory data for determining physical properties (primarily petromagnetic parameters). These results were used to identify areas of the main rock types and to establish the geological sequence and regularities of change of igneous and volcanic rocks of different ages in the study region, which can give a hint for reconstructing the tectono-magmatic evolution of the magmatic arc (batholith) of the Antarctic Peninsula. To evaluate the distribution of the main rock complexes on depth, we performed 2D magnetic modeling.

## Magnetic anomaly of the Antarctic Peninsula batholith

The wide (~120 km) zone of intense magnetic anomalies of the continental margin of Antarctica (Fig. 1) is known as the Pacific Margin Anomaly (PMA; Maslanyj et al. 1991) or the West Coast Magnetic Anomaly (WCMA; Renner et al. 1982), which extends for a distance of about 3800 km. Such magnetic anomalies are rather typical for subduction-related magmatic arcs worldwide (Blakely et al. 2005; Clowes and Hyndman 2002; Saltus et al. 1999; Yegorova et al. 2011, 2022).

The PMA is interpreted as a strongly magnetized chain of batholiths formed in a subduction environment, along the shelf zone of the AP (Leat et al. 1995; Renner et al. 1985; Garrett 1990). It is widely thought that evolution of the Antarctic Plate relates to the accretion of separate domains during progressive subduction in a NE direction of the Phoenix Plate below the western margin of the AP continental plate (Larter et al. 2002), and the AP block represents a Mesozoic–Cenozoic magmatic arc consisting of two or three separate domains (Storey and Garrett 1985; Ferraccioli et al. 2006; Vaughan and Storey 2000; Zheng et al. 2018; Jordan et al. 2020). Ferraccioli et al. (2006) suggested the occurrence within the Antarctic Peninsula batholith of two distinct terranes (Early Cretaceous mafic western arc juxtaposed against a more felsic eastern one). Vaughan et al. (2012) suggested that the two arcs were sutured against the Gondwana margin during the mid-Cretaceous Palmer Land orogenic event. Gravity and magnetic modeling (Yegorova and Bakhmutov 2013) showed that the AP around Anvers Island is an accretionary assemblage formed during subduction in the Mid Cretaceous, where to the AP crust (Gondwana block) an accreted block was welded.

Burton-Johnson and Riley (2015) supported an alternative to the Ferraccioli et al. (2006) and Vaughan et al. (2012) tectonic model of autochthonous continental margin development as an in situ continental arc. A suggestion on extensive Paleogene and Neogene magmatism occurred

along part of an inherited Mesozoic arc/fore-arc boundary was made by Jordan et al. (2014) from higher resolution aeromagnetic surveys across Adelaide Island.

A map of the magnetic field of the Drake Passage and the AP, based on the international IceGrav project in the area between South America, Palmer Land, and South Shetland Islands (Ghidella et al. 2011) shows linear magnetic anomalies on three segments of the extinct Phoenix plate, whereas extended anomalies emphasize the sharp character of the Shackleton fracture zone centered on an adjacent extinct spreading ridge.

The magnetic field obtained for the Bransfield Strait and the northern part of the continental margin of the AP (Catalán et al. 2013) showed that the PMA anomaly splits in places into individual nodes, indicating significant heterogeneities and/or variations in the depths of magnetoactive bodies. Short wavelength positive magnetic anomalies are associated with underwater volcanoes in the central part of the Bransfield Strait.

Interpretation of the PMA in the southeastern part of Palmer Land (Golynsky and Masolov 2000) shows that magnetoactive bodies in the crust would be a series of plutons of different age, composition, and magnetization, limited to 8–10 km depth. The most intensive magnetic anomaly with amplitude of up to 1900 nT can be associated with a magnetized unit having a modeled magnetic susceptibility of 0.09 SI.

In the central part of the AP, between Anvers Island and the northern boundary of the Bransfield Strait, the PMA splits into two branches: a western anomaly with a relatively high magnitude, and a lesser eastern anomaly. The modeling performed here showed that the sources of the PMA are caused by bodies with magnetic susceptibilities of 0.055–0.075 SI, depth of the upper edge in the range of 0–6 km, and of the lower edge up to 20 km (Johnson 1999).

Gravity and magnetic models of the crust and upper mantle were constructed for the central part of the AP using the seismic models as constraints (Yegorova et al. 2011). A magnetic model along profile III in the area of Anvers Island (Fig. 1B; Yegorova and Bakhmutov 2013) attributes the western branch of the PMA to a crustal magnetic body, whereas the eastern branch is caused by a body at the depth of 5–18 km. Their magnetic susceptibilities (0.074 and 0.065 SI correspondingly), characteristic of intrusive rocks of the gabbro group (gabbro-diorites, gabbro-norites; Yegorova et al. 2011; Shpyra et al. 2014), show that two branches of the PMA having formed in the Early Cretaceous within different blocks, i.e., the western branch of the PMA is located within the accreted block, while the eastern PMA within the Gondwana margin of the AP.

So we can assume that high magnitudes of magnetic anomalies due to the presence of mafic rocks in the

magmatic arcs provided valuable information for the deep structure of the crust of West Antarctica.

## Geological setting

The geological setting of the Penola Strait area of the SE part of Wilhelm Archipelago and adjacent coast of the Kyiv Peninsula is shown in Fig. 2. Jurassic, Cretaceous and Paleogene rocks related to AP arc magmatism are well exposed on numerous islands.

The oldest exposures belong to the Antarctic Peninsula Volcanic Group (APVG), previously identified as the Upper Jurassic Volcanic Group (Elliot 1964; Curtis 1966). Recently, it has been proposed to divide the APVG on the Kyiv Peninsula and Wilhelm Archipelago into two geological formations (Mytrokhyn and Bakhmutov 2019). The Kyiv Peninsula Formation (KPF) is the most widespread lithostratigraphic unit in the study area. Exposures on the western coast of Kyiv Peninsula, as well as the Booth and Hovgaard Islands, are of well-stratified pyroclastic rocks including ash tuff, lapilli tuff and tuffite, as well as lesser andesite and basaltic andesite. The volcanics have been subjected to contact-thermal metamorphism and open folding. It is known that APVG ages can vary from Jurassic to Paleogene (Thomson and Pankhurst 1983). An age limit for the KPF is determined from the intrusion of Early Cretaceous granites and diorites (Tangeman et al. 1996). The Argentine Islands Formation (AIF) has a much smaller areal distribution, on the Galindez, Winter, Skua, Black, Leopard, Shelter, Three Little Pigs, Grotto, Corner, Uruguay, Irizar and Fanfare islands of the Wilhelm Archipelago. It is represented by poorly stratified lapilli tuff, pyroclastic breccia and andesite as well as subordinate ash tuff, tuffite, sandstone, mudstone and chert. The AIF has undergone more intense tectonic deformation, contact-thermal metamorphism and metasomatism than the KPF. The AIF volcanism occurred between the Jurassic and Cretaceous periods. The lower age limit coincides with the one accepted for the APVG. The upper age limit is determined by Ar–Ar isotope ages for Paleocene granitoids intruding AIF on the Barchans Islands (Bakhmutov et al. 2013).

Non-metamorphosed intrusive rocks of Antarctic Peninsula batholith are widespread over the Wilhelm Archipelago and Kyiv Peninsula. Due to tectonic uplift and exhumation, both apical and bottom parts of individual intrusive bodies have been exposed. Plutons of gabbroids, diorites and granitoids intersect each other in a complex age sequence. Intrusive relationships make it possible to determine relative geological ages and to reconstruct the general direction of shift in deep magmatism from the Early Cretaceous to the Early Paleogene (Mytrokhyn et al. 2021). Numerous small

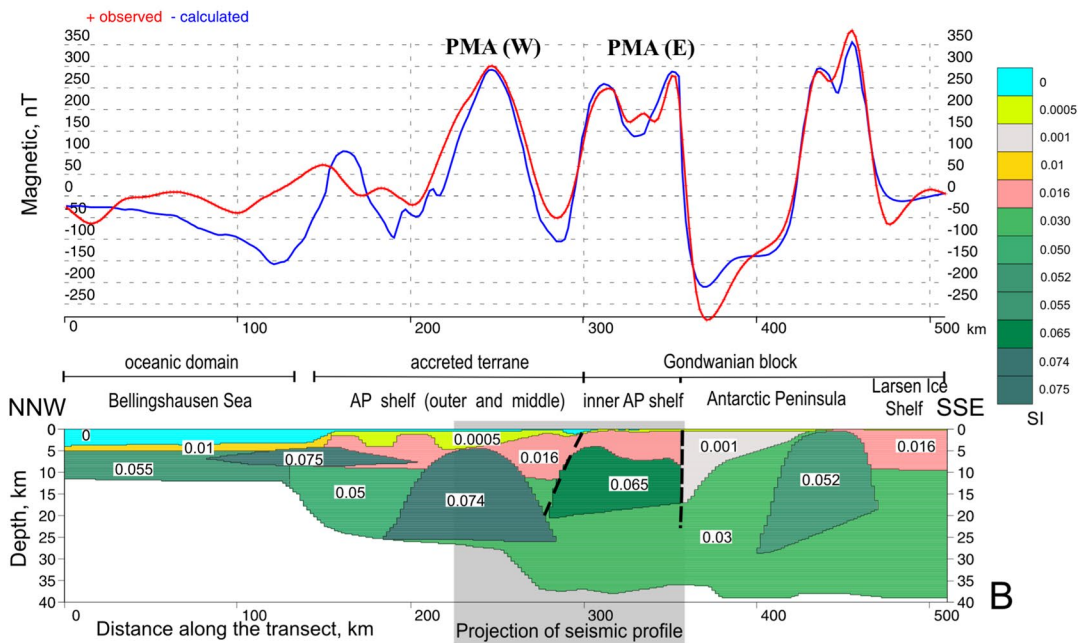
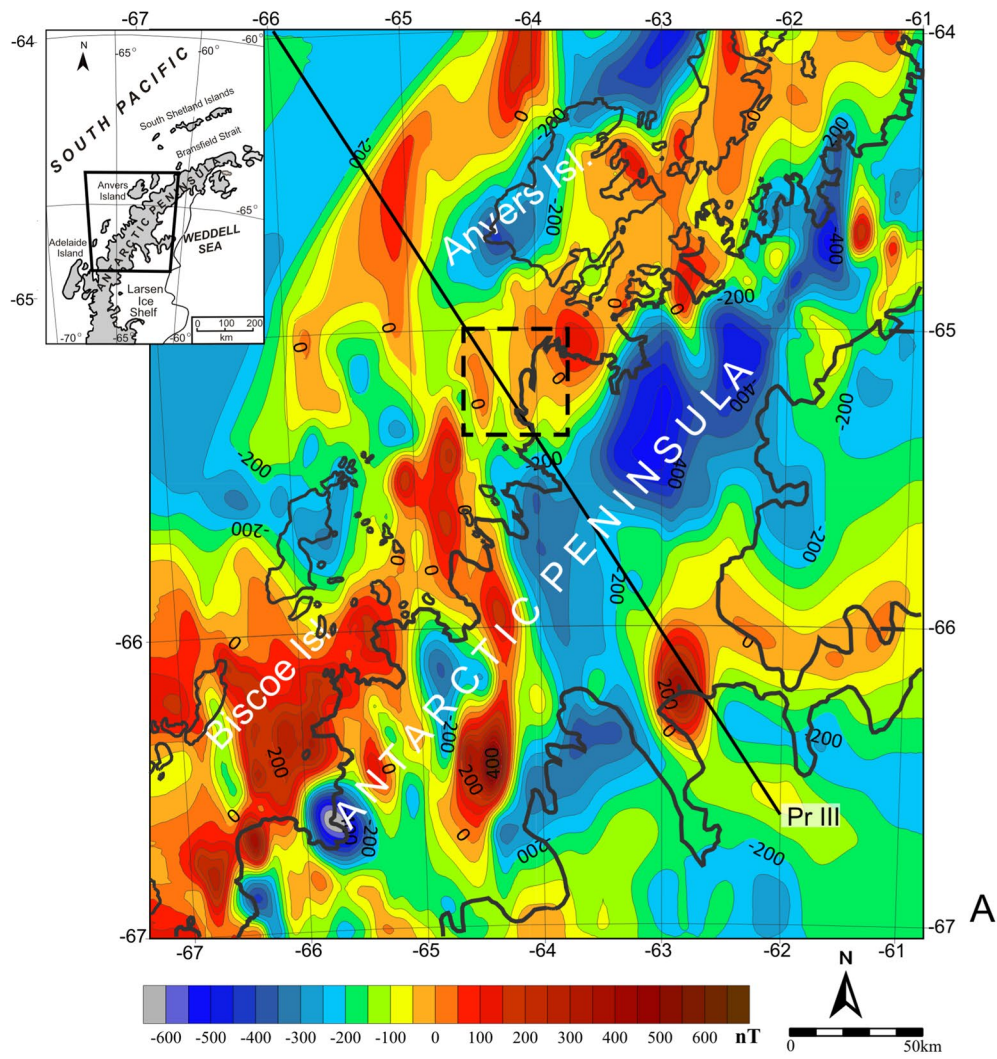


**Fig. 1** The Pacific Margin Anomaly (PMA) over the Antarctic Peninsula (A), with the area of our magnetic survey marked by the dashed rectangle, and the magnetic model of the Earth's crust along profile III (B) crossing the area near Anvers Island from the Bellingshausen Sea to the Antarctic Peninsula (Yegorova and Bakhmutov 2013). The inset map shows the Antarctic Peninsula with the area of the magnetic map in B marked by the black rectangle. The diagonal solid line marks the location of the magnetic model on line III. Numbers on the cross section indicate modeled magnetic susceptibility in SI units

outcrops of gabbro are exposed on the Petermann, Anagram, Berthelot, Hovgaard, Vedel, Roca, Cruls Islands, as well as on the neighboring mainland coastline in Waddington and Girard Bays (Fig. 2). The boundaries of the gabbroid bodies lie below sea level or are covered by permanent snow and ice. Therefore, the sizes of outcropped intrusions can only be estimated from magnetic survey data. The bodies studied are only small exposed parts of much larger intrusive massifs, immersed under the Bellingshausen Sea level or buried under glacial cover. In many places, the gabbro exhibits magmatic layering on various scales. The Tuxen-Rasmussen gabbroid intrusion formed between the accumulation of Jurassic volcanites of the KPF and the intrusion of Upper Cretaceous granitoids. A gabbroid intrusion on the Petermann Islands is the same age (Mytrokhyn et al. 2021). The geological ages of all other gabbroid intrusions remain unclear. Granitoids and diorites are more widespread than gabbroids. They are exposed on many islands, including the Barchans, Forge, Roca, Cruls, Berthelot, Petermann, Vedel, Dannebrog, Hovgaard and Booth Islands, and stretch along the mainland coastline in Duseberg and Moot Point areas, as well as Waddington Bay. Isotopic dating using U–Pb, Rb–Sr and Ar–Ar revealed at least three age groups in the granitoids (Pankhurst 1983; Tangeman et al. 1996; Bakhmutov et al. 2013; Zheng et al. 2018). Early Cretaceous granites outcrop on Rasmussen Island, whereas Late Cretaceous granodiorites are exposed on Mount Demaria and Petermann Island. Paleogene granodiorite plutons are widespread on the Barchans, Forge and Booth Islands. The formation of diorite intrusions took place between the Early Cretaceous and the Paleocene (Mytrokhyn et al. 2021).

Numerous mafic dykes intrude APVG and AP batholith rocks in the Wilhelm Archipelago and on the adjacent mainland (Elliot 1964; Mytrokhyn et al. 2022). Compared to plutonic rocks, the areal proportion of dyke bodies is insignificant. The dykes are mainly basalt, diabase, microgabbro and microdiorite, and their distribution and orientation are controlled by the NE-striking Lemaire–Penola regional fault zone (Fig. 2). Mutual cross-cutting of dykes and dating of host rocks demonstrated at least two stages of dyke intrusion in the Mesozoic and Cenozoic.

## Methods and results

### Magnetic properties of rocks

Magnetic properties of rocks depend on conditions of their formation and subsequent changes. In addition to main geological factors (thermodynamic conditions of rock formation, depth of the magma chamber, the rate of effusion and crystallization, manifestation of metamorphism impact, etc.), other factors such as concentration, composition, structure, magnetic fabric, can also be considered as key factors determining the magnetic properties of rocks. The latter primarily reflects the partitioning of iron between strongly magnetic oxides and weakly magnetic material. This partitioning depends on chemical composition, iron oxidation ratio, and conditions of petrogenesis (e.g., Clark 1997; Frost 1991). It is generally accepted that among all Fe–Ti oxides, spinel magnetite ( $\text{Fe}_3\text{O}_4$ ) is the key mineral that determines the magnetic susceptibility of rocks. Thus, the magnetic susceptibility is an indicator of the content of ferromagnetic minerals of the titanomagnetite series. Because magnetite is the strongest magnetic mineral, the measurements of magnetic susceptibility of highly magnetized rocks are a direct indicator of the average magnetite content of the rocks. Subsequent and secondary processes also affect the content of titanomagnetite minerals. Some of them (chloritization, albitization, etc.) lead to the destruction of primary magnetic minerals. Vice versa, serpentinization, and frequent biotization, facilitate the formation of magnetite in rocks.

In general, the mafic rocks, due to the higher iron content, contain more minerals of the titanomagnetite series than the felsic ones. The concentration of magnetic minerals in igneous rocks is affected by redox conditions, which are closely related to tectonic setting and magmatism. In addition, the concentration of magnetic minerals also has a certain relationship with the depth of magma formation. Under the conditions of the Earth's crust and upper mantle, the maximum depth of existence of magnetic minerals is estimated at 50–60 km.

The magnetic parameters of the Antarctic Peninsula rocks are known from Garrett (1990), Wendt et al. (2013). The magnetic analyses conducted by the authors include determinations of the magnetic susceptibility (MS) and initial natural remanent magnetization (NRM) on more than 500 samples of plutonic and volcanic rocks exposed on the Kyiv Peninsula and adjacent islands (Bakhmutov and Shpyra 2011; Bakhmutov et al. 2013; Shpyra et al. 2014). All samples were collected from blocky, solid and visually unaltered rocks on the sites that covered the maximum accessible (ice-free) area. The locations of sites are presented on Fig. 1 in (Bakhmutov and Shpyra 2011).

The MS of samples was measured by Geofyzika Brno Kappameter MFK-1B. The initial NRM of oriented specimens cut out from these samples was measured by a JR-6 spinner magnetometer. The data were analyzed and compared with the results of geochemical studies of magmatic rocks from different locations. On the TAS diagram (total alkali vs. silica  $\text{SiO}_2-(\text{Na}_2\text{O} + \text{K}_2\text{O})$ ) the content of  $\text{SiO}_2$  varies from 40 to 70% (Suppl. Figure 1). Three groups of maximum concentration related to gabbroids, diorites, and granitoids could be allocated on the TAS diagram for the silica content. Based on these geochemical data and geological field observations, intrusive rocks were divided into three groups depending on the differences in magnetic parameters—gabbroids, diorites, and granodiorites-granites (Suppl. Figure 2).

The mafic rocks (gabbroids group) have the highest values of mean susceptibility and NRM-0.068 SI and  $2.08 \text{ Am}^{-1}$ , respectively (Suppl. Table). The diorites are characterized by half of the mean MS values ( $0.036 \text{ SI}$ ) and much lower mean NRM ( $0.3 \text{ Am}^{-1}$ ). The rocks, which we attribute to granitoids, have two or three times lower mean MS and NRM values ( $0.02 \text{ SI}$  and  $0.1 \text{ Am}^{-1}$ , respectively).

The available NRM measurements for the intrusive rocks of this region (Grunow 1993; Bakhmutov and Shpyra 2011; Poblete et al. 2011) show that the prevailing NRM direction is normal, i.e., parallel to the recent Earth's magnetic field. The  $Q$ -ratio (the ratio of induced to remanent magnetizations) is predominantly  $< 1.0$  (Table 1). Only in gabbroids it can be  $> 1.0$ , which indicates that the NRM can account for a significant part of the total magnetization.

The volcanic rocks of the APVG are represented mainly by lithic tuffs, andesites, rhyolites, dacites and characterized by minimal values of magnetic parameters. The known volcanic succession of the Penola Strait area is characterized by large differences in magnetic susceptibility, even for similar rock types. In general, the mean values of magnetic susceptibility ( $0.0044 \text{ SI}$ ) and NRM ( $0.03 \text{ Am}^{-1}$ ) of the volcanic rocks are, respectively, one and two orders of magnitude lower than those of gabbro. The lowest values of magnetic susceptibility belong to dacite tuffs from the Argentine Islands (mean  $0.00036 \text{ SI}$ ).

For further modeling on the Pr1 profile, the normal polarity was assigned to magnetic bodies. The magnetic parameters of the rocks outcropped near the Pr1 profile are presented in Table 1.

### Boat magnetic survey technique

In the case study, when the geology is known from the outcrops on the ice-free islands and along the coastline of the adjoining part of the AP, the informative method is a magnetic survey, followed by the construction of a magnetic anomaly map. Offshore, near the UAS “Akademik

Vernadsky” area, magnetic survey was carried out by the authors of the paper during several summer field seasons (2005–2019 yy) using Zodiac boats. Some early results of the survey for several profiles were presented by Orlyuk and Romanets (2009). In the course of further research, the network of profiles was significantly expanded. The current distribution of survey tracks is shown in Fig. 3.

Magnetic surveying was carried out using a PMP-8 (or MMP-203) proton magnetometer mounted on the bow of a Zodiac-type boat (Fig. 4). A distance of about 5 m from the sensor to the engine (Johnson-40) on the rubber boat Zodiac prevents the magnetic field being affected by the metal engine. Logging of magnetic induction values and GPS coordinates (by Garmin GPSMAP) was performed every 10 s at a boat speed of 10 km/h. To monitor diurnal geomagnetic variations the data from Argentine Islands magnetic observatory (AIA) at “Akademik Vernadsky” station was applied.

### Mapping the magnetic field of the study area

#### Data processing and correction

The correction for the magnetic field variation was applied to the initial data:

$$B_i = B_{ci} - \delta B_i, \quad (1)$$

where  $B_i$  is the magnetic field strength value at the  $i$ -th point that takes into account variations from external sources of the magnetic field,  $B_{ci}$  is the observed value of the total vector modulus of the magnetic field at the  $i$ -th point,  $\delta B_i$  is the magnitude of the magnetic field variation at the time of the  $i$ -th observation point, calculated by the formula:

$$\delta B_i = B_{UASi} - B_m, \quad (2)$$

where  $B_{UASi}$  is the value measured by scalar magnetometer at the AIA observatory at the time of the observation point measurement,  $B_m$  is the daily average measured at the observatory.

Accounting for the standard component ( $B_{0i}$ ) of the international geomagnetic field was performed using the International Geomagnetic Reference Field (IGRF) online calculator (<https://www.ngdc.noaa.gov/geomag-web/#igrfgrid>) on a grid with a  $1^\circ$  step in latitude and longitude for the area limited by  $60\text{--}70^\circ \text{ S}$  and  $60\text{--}70^\circ \text{ W}$ . The resulting  $B_{0i}$  values were interpolated using Surfer by Golden Software and gridded with a  $0.01$  degree grid step on longitude and latitude. The obtained  $B_{0i}$  values have already taken into account the secular variations of the magnetic field by automatic interpolation.

The values of the anomalous magnetic field at the measurement points were calculated by the formula:

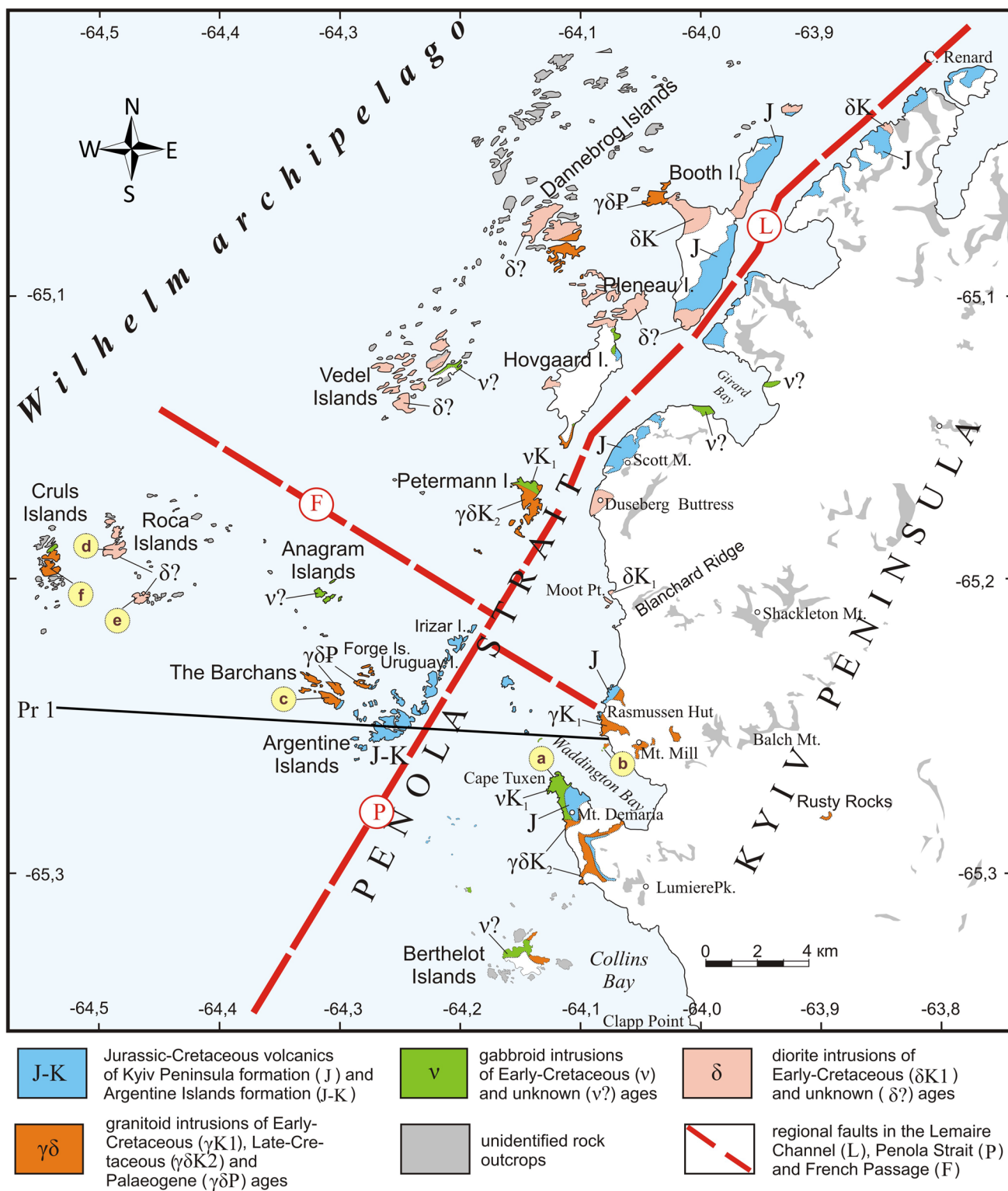


**Fig. 2** Geological map of Wilhelm Archipelago and the adjacent coast of the Kyiv Peninsula (Mytrokhyn and Bakhmutov 2021). The black line shows the position of the Pr1 profile. Yellow circles with letters indicate the sampling points for magnetic parameters measurements (Table 1)

$$B_{ai} = B_i - B_{oi} \quad (3)$$

The data of all surveys of the anomalous magnetic field were put together in a single table that contains the coordinates and the values of  $B_{ai}$  of the points. This compiled the data base for the construction of the anomalous magnetic field map for the study area (Fig. 5).

### Magnetic field of the study area

The distribution of the anomalous magnetic field  $B_{ai}$  of the Argentine Islands with the adjacent area, including the western part of the AP, shows a wide range of magnitude changes from 3200 nT to –1400 nT (Fig. 5). In the central part of the study area, there is distinguished a band of negative values (from 0 to –500 nT) of ~NE extension, which starts in the north near the islands of Booth and Hovgaard, and Girard Bay on the AP. It follows the area of Petermann Island, passes through the Argentine Islands, and the Barchans Islands, where the strip reaches its maximum width and goes further south to about the latitude of 65.35°S. A local area of a negative magnetic field is distinguished in the Cape Tuxen area (Demaria Mount) on the AP coast. A large area of negative values lies in the southern segment of the map south of Berthelot Islands, up to latitude 65.48°S (Fig. 5).

To the west and north–west of the band of negative values of  $B_{ai}$ , there is a band of positive values of magnetic field (from 0 to 500 nT) of the same NE extension with some local anomalies of high intensity (700–1500 nT) and various configurations.

Between the described NE band of the negative values and the area of the negative field in the southern segment of the map (south of the Berthelot Islands), there is another bizarre stripe of positive magnetic field (Fig. 5). It begins in the south at latitude 65.42°S and passes northwards along the Berthelot Islands, Cape Tuxen, Waddington Bay, and Moot Point. This band includes more intense anomalies inside with magnitudes in the range of 1000–2000 nT. Among them one can see three anomalous regions of positive values of  $B_{ai}$ : (1) the region near Cape Tuxen and Moot Point that continues westwards in the shallow water to about the longitude of 64.2°W; (2) the Berthelot Islands area that extends to 64.3°W longitude; and 3) the shallow water domain in the southern part the area, located between 65.35°–65.44°S and 64.3°–64.2°W (Fig. 5).

Magnetic maps of different wavelengths were obtained and constructed by transformations of the anomalous magnetic field  $B_{ai}$  (Fig. 5). To highlight the structure of the magnetic field from the deep magnetic sources, we undertook the averaging of the  $B_{ai}$  field with a 5 × 5 km cell and obtained the long wavelength component  $B_{ai}$  (Fig. 6). The latter could

be caused mainly by rocks of the lower and middle parts of the crust. The short wavelength component (Fig. 7), calculated as the difference between the original  $B_{ai}$  and its long wavelength component (Fig. 6), is caused by magnetic inhomogeneities located in the basement and upper crystalline crust at the depths range of 0.2–13.0 km (Fig. 7).

The described above areas of the anomalous magnetic field, in the form of two bands of positive magnetic field and two stripes of the negative magnetic field of general NE strike, have a good correlation with the long wavelength (regional) component of the magnetic field (Fig. 6), where the maximum magnitudes (> 1000 nT) highlight the anomaly near Cape Tuxen and Moot Point on the AP coast. Within the south-eastern band of positive anomalies (Fig. 6), the three mentioned above short wavelength (local) magnetic anomalies are seen in the Cape Tuxen and Moot Point area, near the Berthelot Islands, and in the southern area between 65.35°–65.44° S and 64.3°–64.2° W (Fig. 7). The stripes of the negative magnetic field correspond well with low magnetic volcanics. Whereas the bands of the positive magnetic field could be due to the intrusive complex of the AP batholith, represented by high magnetic granodiorites, diorites, and gabbroids. Local anomalies within the areas of the positive magnetic field (Fig. 7) may be caused by bodies of gabbro and gabbro–norites.

### Two-dimensional magnetic modeling

#### Parameterization of the model and methodology of the modeling

To study the structure of the upper part of the Earth's crust and to determine the shape of magnetic sources and their magnetic parameters, we performed magnetic modeling on the Pr1 profile (Fig. 8) extending almost across the magnetic anomalies strike (Figs. 5, 6, 7).

For 2D magnetic modeling, we used the software developed by Zavoytskiy (1978) and Kovalenko-Zavoytskiy and Ivashenko (2006) at the Institute of Geophysics of the National Academy of Sciences of Ukraine for solving the direct magnetic problem for bodies approximated by prisms. The prisms define the areas of constant magnetic susceptibility. During the modeling we set the extension of the structures crossed by the profile. The magnetic bodies are placed mainly in the upper crust interval, bounded below by the Curie isotherm, which is estimated for the AP continental margin at the depth of approximately 20–25 km (Johnson 1999). During the modeling, the geometry of the crystalline crust bodies and their magnetic susceptibilities should be determined.

The input data we used to construct the magnetic model include the plots of the anomalous geomagnetic field  $B_{ai}$ , the



depth of the crystalline basement, and the laboratory data on the magnetic susceptibility and NRM vector directions of rock samples (see Section “Magnetic properties of rocks”). The NRM direction (inclination  $I^\circ$  and declination  $D^\circ$ ) was taken into account from the paleomagnetic studies (Table 2 in (Bakhmutov and Shpyra 2011)). Further refinement of the models was achieved with a better correspondence between the calculated and observed magnetic fields by introducing the corrections in the geometry of bodies and their susceptibilities. The values of magnetic susceptibilities of key units of the model were counter checked with the linear inversion option that is offered by the software used.

## Results

According to velocity modeling on the deep seismic marine profiles (Šroda et al. 1997; Grad et al. 2002), the continental margin of the AP has a thin (0.2–1.5 km) sedimentary cover above the crystalline crust consisting of the upper, middle and lower crust with velocities of 6.3–6.4, 6.6–6.8, and 7.1–7.2 km/s correspondingly. Depths to the Moho are in the range of 36–42 km. The largest thickness of the crust was found in the Adelaide, Bisco, and Anvers Islands (Grad et al. 2002; Janik et al. 2006, 2014). Westwards, in the direction of the Bellingshausen Sea, the Moho depths decrease to 25–28 km.

In the first approximation, the observed geomagnetic field  $B_{ai}$  of the study area represents a set of prism-shaped magnetic field sources. The depths to the upper edges (boundaries) constitute the first hundreds of meters, and the lower limit of magnetic sources is in the range of 4–12 km (Golynsky and Masolov 2000; Jordan et al. 2014; Soloviev et al. 2018). To parameterize the magnetic properties of the bodies we used the laboratory data obtained at the sampling points of the rocks in the study area (Yegorova et al. 2011; Bakhmutov et al. 2013; Shpyra et al. 2014). The magnetic

model on the Pr1 profile consists of 12 bodies with depths to the upper edge of 0.2–0.5 km, and their lower limits located at a depth of 12 km (Fig. 8). The magnetic susceptibility of the sources varies from 0.005 to 0.13 SI (Fig. 8, Table 2).

The modelings performed on the Pr1 profile allow to identify two groups of magnetic bodies (bodies 1–5 and 7–10 in Fig. 8 and in Table 2), which cause the western and eastern bands of positive anomalies with amplitudes of 500 and 850 nT, respectively (Figs. 5 and 7). The magnetic susceptibility of these bodies, which have a predominant shape of trapezes and prisms, and a vertical dip, varies in the range of 0.03–0.13 SI (Table 2). This indicates that these bodies belong to the gabbro group rocks. Between these two bands of magnetic maxima above the gabbroid bodies, there is a quite wide magnetic minimum of  $\sim -200$  nT, which is caused (explained) by volcanic rocks with a magnetic susceptibility of 0.005 SI (Fig. 8, Table 2).

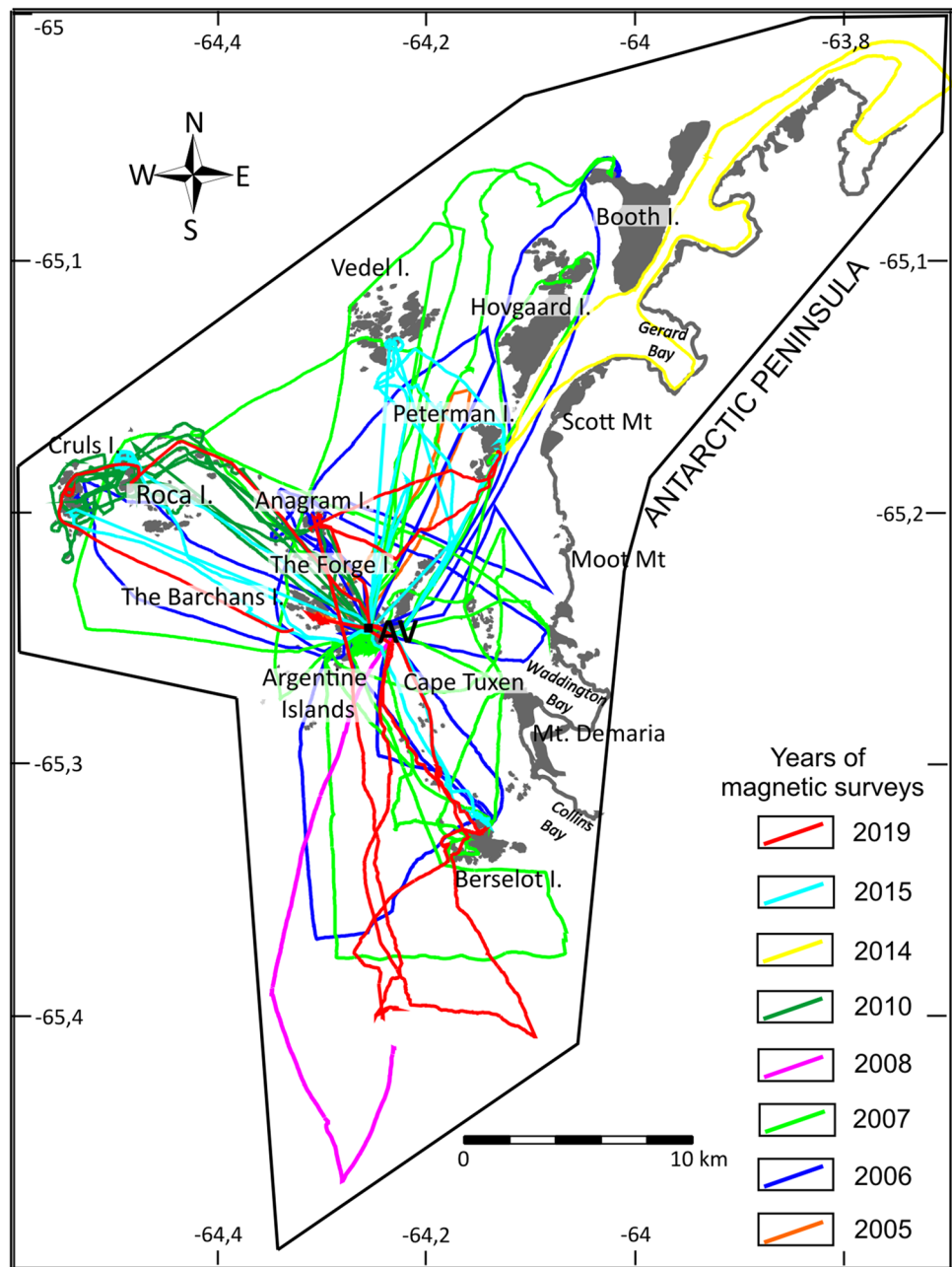
## Interpretation of the magnetic map

As noted above, the anomalous magnetic field of the study area is represented by the positive and negative field bands of the general NE extension, within which anomalous domains and individual anomalies of different shapes and sizes are distinguished (Figs. 5, 6, 7). The anomalous magnetic field is strongly differentiated, with anomalies of different size, amplitude, configuration, and extent due to the significant distribution of effusive and igneous formations of the AP. They include all petrographic representatives of volcanic rocks and the gabbro-diorite-granite association. Plutons of different ages intersect in a complex sequence. Taking into account the available information on the composition and age of rocks and magnetic modeling data based on magnetic parameters, it is possible to analyze the magnetic field with the assessment of rock types.

**Table 1** Magnetic parameters of rocks in the area of the Pr1 profile. The range (underlined) and mean values are given for NRM, magnetic susceptibility, and  $Q$ -ratio. The locations of sampling sites a-f are shown in Fig. 5

No	Sampling location	Rocks	Number of samples	Natural remanent magnetization (NRM), $\text{Am}^{-1}$	Magnetic susceptibility (MS), SI	$Q$ -ratio
a	CapeTuxen (64.11°W, 65.27°S)	Gabbro	19	<u>0.8–4.7</u> 3.0	<u>0.04–0.25</u> 0.13	<u>0.3–1.1</u> 0.6
b	Rasmussen island (64.079°W, 65.257°S)	Gabbro	26	<u>0.43–4.4</u> 1.8	<u>0.007–0.08</u> 0.047	<u>0.26–2.67</u> 0.11
c	The Barchans (64.32°W, 65.23°S)	Diorite	24	<u>0.04–0.4</u> 0.17	<u>0.017–0.04</u> 0.03	<u>0.04–0.34</u> 0.15
d	Roca islands (64.48°W, 65.19°S)	Diorite	10	<u>0.05–0.53</u> 0.26	<u>0.015–0.084</u> 0.055	<u>0.02–0.2</u> 0.125
e	Roca islands (64.458°W, 65.206°S)	Diorite	6	<u>0.04–0.26</u> 0.11	<u>0.032–0.047</u> 0.04	<u>0.03–0.14</u> 0.06
f	Cruls islands (64.54°W, 65.19°S)	Diorite, gabbro	14	<u>0.39–0.98</u> 0.6	<u>0.006–0.03</u> 0.015	<u>0.39–2.83</u> 1.23

**Fig. 3** Scheme of magnetic survey tracks for 2005–2019 yy in the studied area of the Wilhelm Archipelago. Location of UAS “Akademik Vernadsky” is marked by AV



### Preliminary geological interpretation of the magnetic map

In the magnetic field, one can see two bands of the negative magnetic field (of a complex configuration) of general N-NE strike, parallel to the APV shoreline (Fig. 5), which may be caused by the oldest rocks belonging to the APVG. The western strip passes through the islands of Booth, Hovgaard, Petermann, and the Argentine Islands. It then continues southward to 65.35°S. The second region of volcanic rocks is located in the southern part of the region (south of the Berthelot Islands).

Between the two bands of negative magnetic field above the volcanics and west of the western band of volcanics is a region of positive magnetic field anomalies associated with diorite–granodiorite complex. The latter is represented by a large variety of igneous rocks from medium to acidic composition—diorites, granodiorites and granites of different composition. Since the values of magnetic parameters of diorites and granitoids differ slightly, we combined them into a single group with average values of magnetic susceptibility of 0.02–0.03 SI and the NRM of 0.1–0.3 Am<sup>-1</sup> (see Supplementary Table and Fig. 2 in the Supplement showing the MS and the NRM for the granitoids



**Fig. 4** Boat Zodiac with set up of proton magnetometer PMP-8 used for the magnetic survey. Shows the mounting of the magnetometer sensor on the Zodiac rubber boat, and a panel of PMP-8 (top right

corner) in (a), and conducting the magnetic survey in the shelf area where the magnetometer sensor moved forward and not being affected by the magnetic noise from the engine on the boat stern (b)

(127 samples) and diorites (131 sample). Modeled MS of 0.005 SI for body 10 could be explained by leucocratic granite (Table 2), which is close to MS minimal values for the group of granitoids (Supplementary Table). This corresponds with the modeled parameters on the Pr1 profile that show magnetic susceptibility and the NRM values in the shallow granitic body (body number 10 in Fig. 8) to be 0.005 SI and  $0.1 \text{ Am}^{-1}$ , respectively.

These rocks are mapped in the outcrops on the islands of Booth, Hovgaard, Pleneau, Barchans-Forge, Petermann, Dannebrog, Vedel, Roca, Cruls, Berthelot, and some small cliffs above sea level. Along the coast, diorites and granitoids come to the surface near Duseberg Buttress, Moot Point, Waddington Bay, and Cape Tuxen (Figs. 2, 9). On the Booth Island, the intrusive contact of diorites and Jurassic volcanites of KPF was found, and the diorites themselves were intruded by Paleogene granitoids (Mytrokhyn et al. 2021). The Early Paleogene dating, recently obtained by Zheng et al. (2018) for the quartz diorites of Booth Island, is probably rejuvenated. U–Pb isotopic dating of zircons from Moot Point diorites indicates their Early Cretaceous age (Tangeman et al. 1996).

The distribution of granitoid intrusions is comparable with that of diorite. Among granitoids, granodiorites are the most common, while granites and tonalites are less common. Isotopic dating distinguishes at least two age groups of granitoids—Late Cretaceous and Paleogene (Mytrokhyn et al. 2021). Late Cretaceous granitoids were found only on Petermann Island. Granitoids on the islands of Barchans, Forge and Booth have Paleogene age. All other manifestations of granitoid magmatism on the islands of the Wilhelm Archipelago remain undated.

According to field observations, granitoids are younger than gabbroid and diorite plutons. Age relationships of gabbroids and diorites are more complex. In some cases,

they have features of magmatic mixing and they were crystallized almost simultaneously. In other cases, diorites are embedded in fully crystallized gabbroids.

In the positive magnetic field of granitoids, there is a large number of local maxima (up to  $\geq 800 \text{ nT}$  in amplitude) which correspond to the gabbro group. The latter is represented by a wide range of rocks from ultramafic species to gabbro-norites, gabbro, and anorthosites. Sometimes they are observed as layered intrusions (Artemenko et al. 2013).

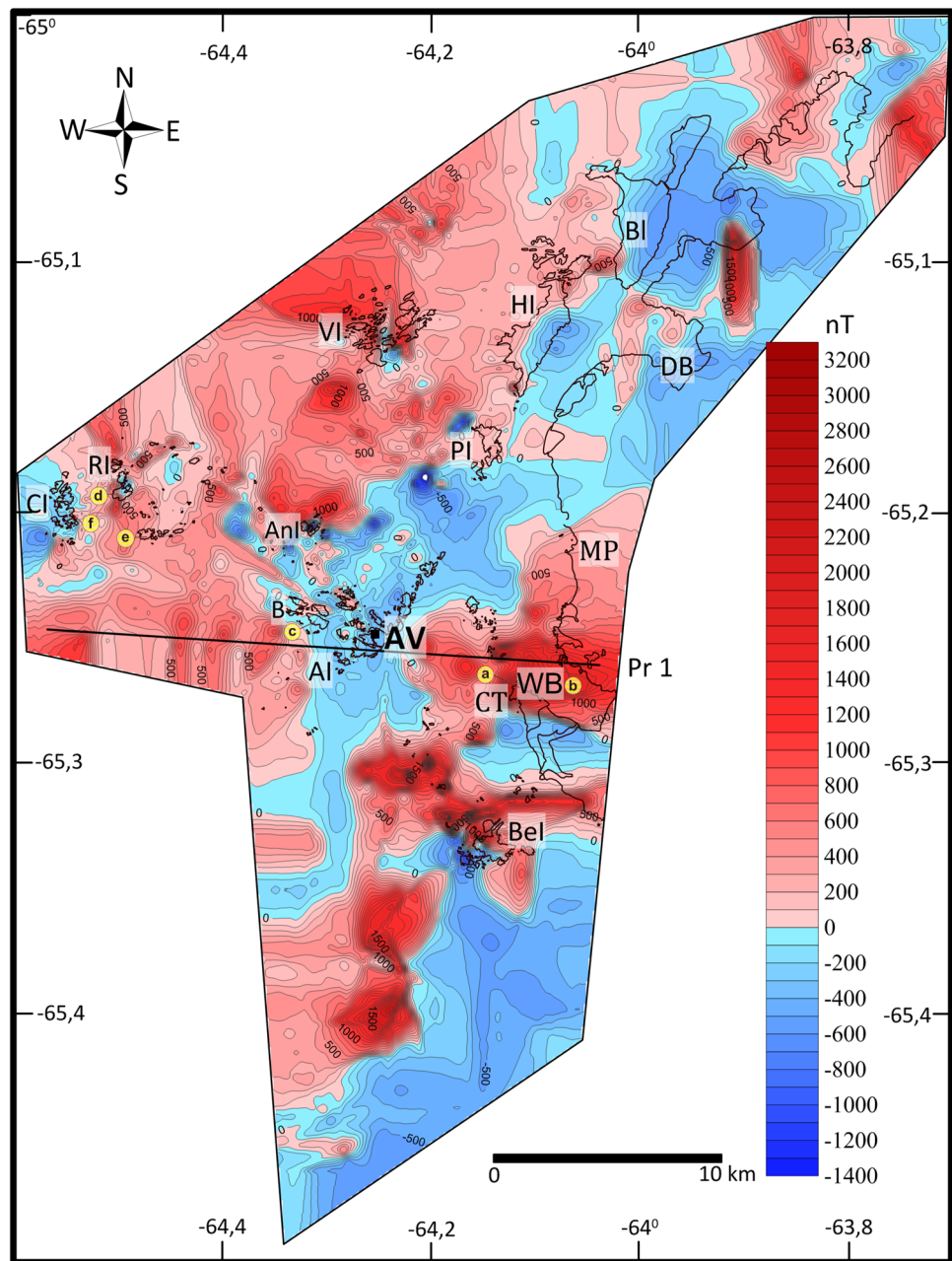
Gabbroid intrusions of the Wilhelm Archipelago occupy much smaller areas compared to granitoids. The interpretation of anomalies as caused by gabbroids is confirmed by mapping their outcrops on the islands of Berthelot, Anagram, Petermann, Hovgaard, Vedel, Cruls, as well as along the coast of the Girard Bay, Waddington Bay, and Cape Tuxen (Figs. 2 and 9). None of the mapped gabbroic bodies could be outlined on all sides. Therefore, data on their size are incomplete, but can be estimated from magnetic survey data (Figs. 5, 6, 7).

Our modeling of the Pr1 profile (Fig. 8, Table 2) shows that the gabbroid bodies are located in the upper crust to a depth of  $\sim 12 \text{ km}$  and have a magnetic susceptibility of 0.031–0.10 SI, which corresponds to the range of MS of gabbroids (Suppl. Table).

### Fault tectonic

The tectonic lineaments in the magnetic field exhibit such features as axes of magnetic minima, gradient zones, linear anomalies and their chains, and chains of local anomalies. Due to these patterns, tectonic faults were identified in the magnetic field pattern in the study area.

**Fig. 5** Map of the anomalous magnetic field of the Wilhelm Archipelago shelf zone, built on the basis of magnetic surveys for 2005–2019 yy. Isolines are in nT. The black line shows the position of the Pr1 profile, chosen for magnetic modeling (Fig. 8); yellow circles with letters indicate the sampling points for magnetic parameters measurements (Table 1). AV-“Akademik Vernadsky” station (black square), AnI-Anagram island, AI-Argentine islands, B-The Barchans islands, BeI-Berthelot islands, BI-Booth island, CI-Cruls islands, GB-Girard Bay, HI-Hovgaard island, WB-Waddington Bay, CT-Cape Tuxen, MP-Moot Point, PI-Petermann island, RI-Roca islands, VI-Vedel islands

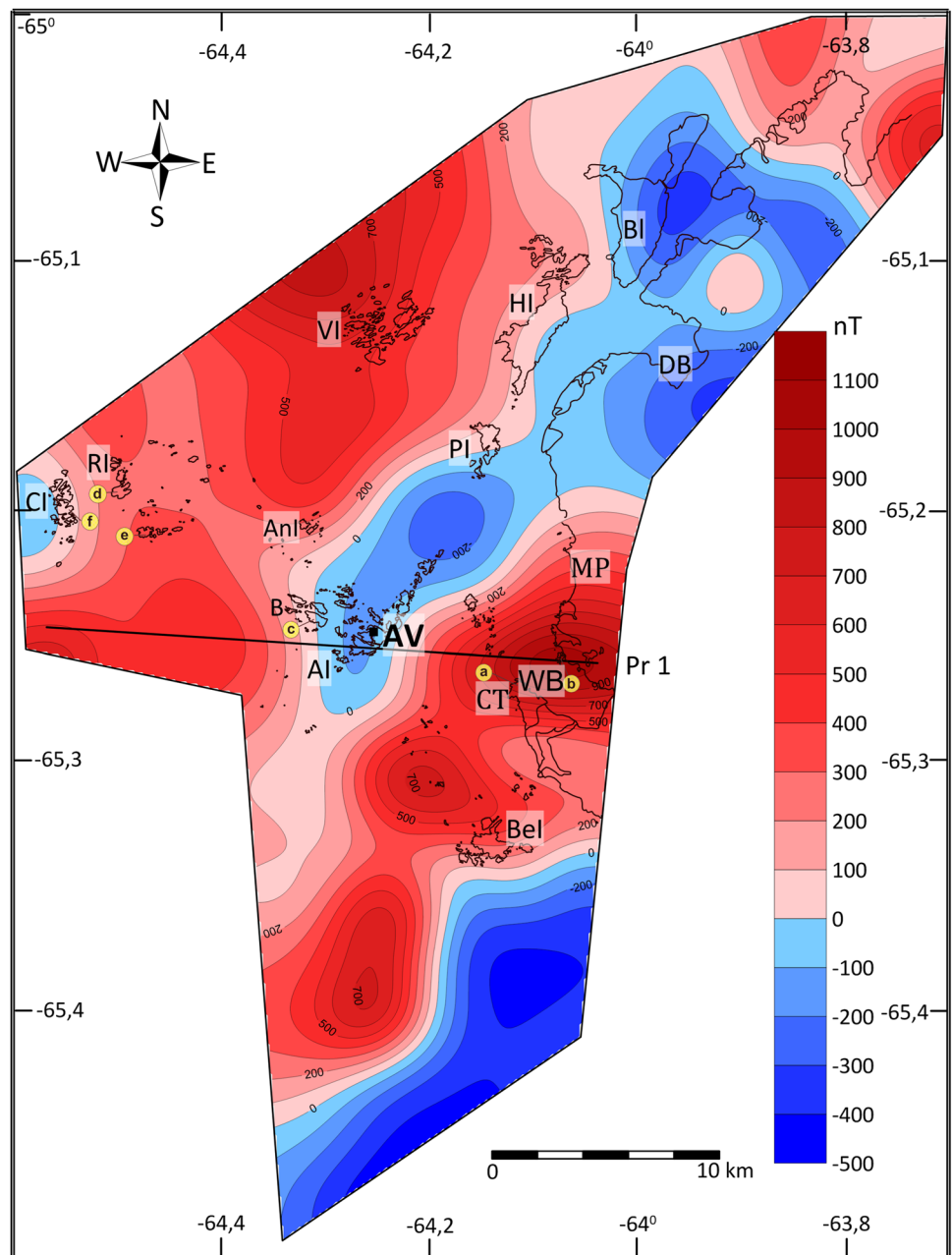


Analysis of the anomalous magnetic field map revealed an orthogonal system of NW and NE tectonic faults (Fig. 10). The NE fault extends subparallel to the AP coast along the Penola Strait (Penola Strait Fault). In the north, it passes through the Booth and Hovgaard Islands, the Petermann Islands, along the chain of the Argentine Islands of general NE strike, and southward along the magnetic minimum axis at longitude 64.3°W longitude (Fig. 10). For most of its extent, from Booth Island to the Argentine Islands, this fault coincides with that identified from the bathymetry data (Maksymchuk et al. 2009). Its position in Fig. 9 differs from that in Fig. 2 south of the Argentine Islands, where,

according to the magnetic data, it is drawn along the N–S minimum.

The second fault system of NW strike includes three faults in the central part of map and one fault crossing the northern part of the Booth Island (Fig. 10). They intersect the NE fault of the Penola Strait, and are most likely transform faults as they locate sub-orthogonally to both the Penola Strait fault and the AP coastline. Note that the same NW strike is characteristic of the well-known Shackleton and Hero transform faults that limit the South-Shetland block at the northern part of the AP (Birkenmajer 1994). The central fault of the NW faults corresponds to the Barchans fault (Fig. 10), which crosses the Barchans and the Argentine

**Fig. 6** Long wavelength (regional) component of the anomalous magnetic field of the study area. For the explanations of symbols see Fig. 5



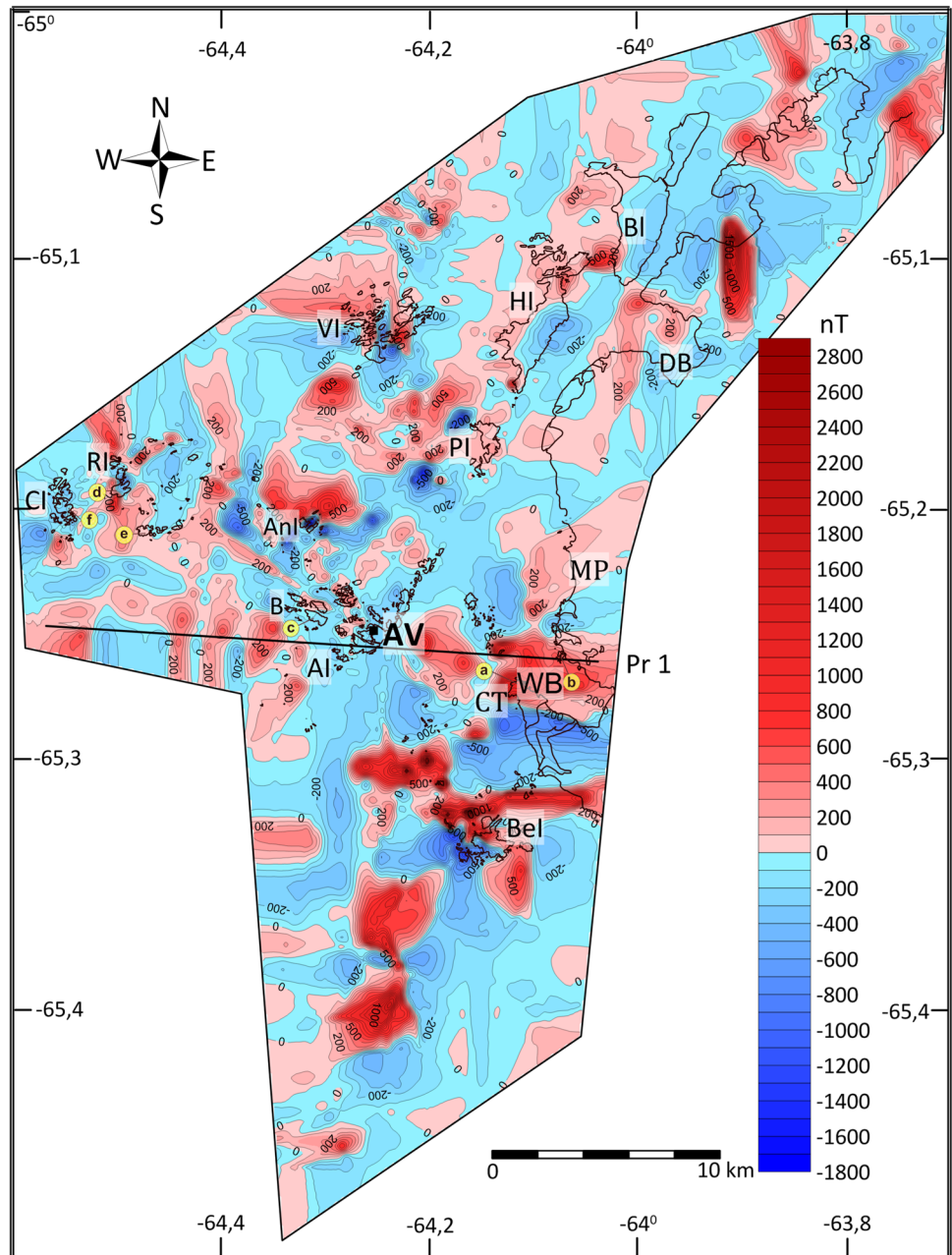
Islands. It is traced further southeast along the gradient termination of the magnetic maximum at Cape Tuxen (Fig. 10). To the north of the Barchans fault and parallel to it, there is another fault of the same strike, running near the northern termination of the Argentine islands (Fig. 10) and corresponding to the fault marked with “F” in Fig. 2. The position of the southernmost transform fault is defined by a sharp gradient of positive anomalies at the southern end of the Berthelot Islands area (Fig. 10).

The isolation of the sub-orthogonal system of NE and NW faults is quite natural in terms of paleotectonic reconstructions and general geodynamic evolution of the

region as part of a continental margin whose tectonic and magmatic activity ended relatively recently (Late Cretaceous–Paleogene), e.g., Larter and Barker (1991), Vaughan and Pankhurst (2008), Zheng et al. (2018). The NE fault is older than the transform NW faults. The former occurs in a band of the ancient weakly magnetic rocks of the volcanic complex along the Penola Strait (Fig. 2). Their formation is most likely related to the Jurassic breakup of Gondwana and the separation of Antarctica from it (Riley et al. 2001, 2017; Pankhurst et al. 2000).

We interpret the NW strike-slip faults as younger transform faults associated with the subduction-collision stage

**Fig. 7** Short wavelength (local) component of the anomalous magnetic field of the study area. For the explanations of symbols see Fig. 5



of an active continental margin evolution during the Early Cretaceous-Paleogene as a result of subduction of the Proto-Pacific Plate (Phoenix Plate) under the AP continental shelf, which was accompanied by melting of AP gabbro-granitoid series rocks. The same nature and extent are characteristic of the known Hero and Shackleton transform faults in the northern part of the AP, delimiting the South Shetland Islands block from the northwest and northeast, where subduction is still thought to be active (Pelayo and Wiens 1989; Stacey et al. 2003).

## Conclusions

- (1) Magnetic surveys of the offshore area near the Argentine Islands and adjacent islands have enabled us to build maps of magnetic field anomalies, including regional and local components. This is the first time such detailed maps have been compiled in the SE part of Wilhelm Archipelago, West Antarctica. This region comprises a great variety of volcanic and magmatic rocks with differing magnetic properties, producing various magnetic field anomalies. These include volcanic series of the Antarctic Peninsula (andesites, diabbases, basalts, rhyolites, dolerites, dacites) of Upper

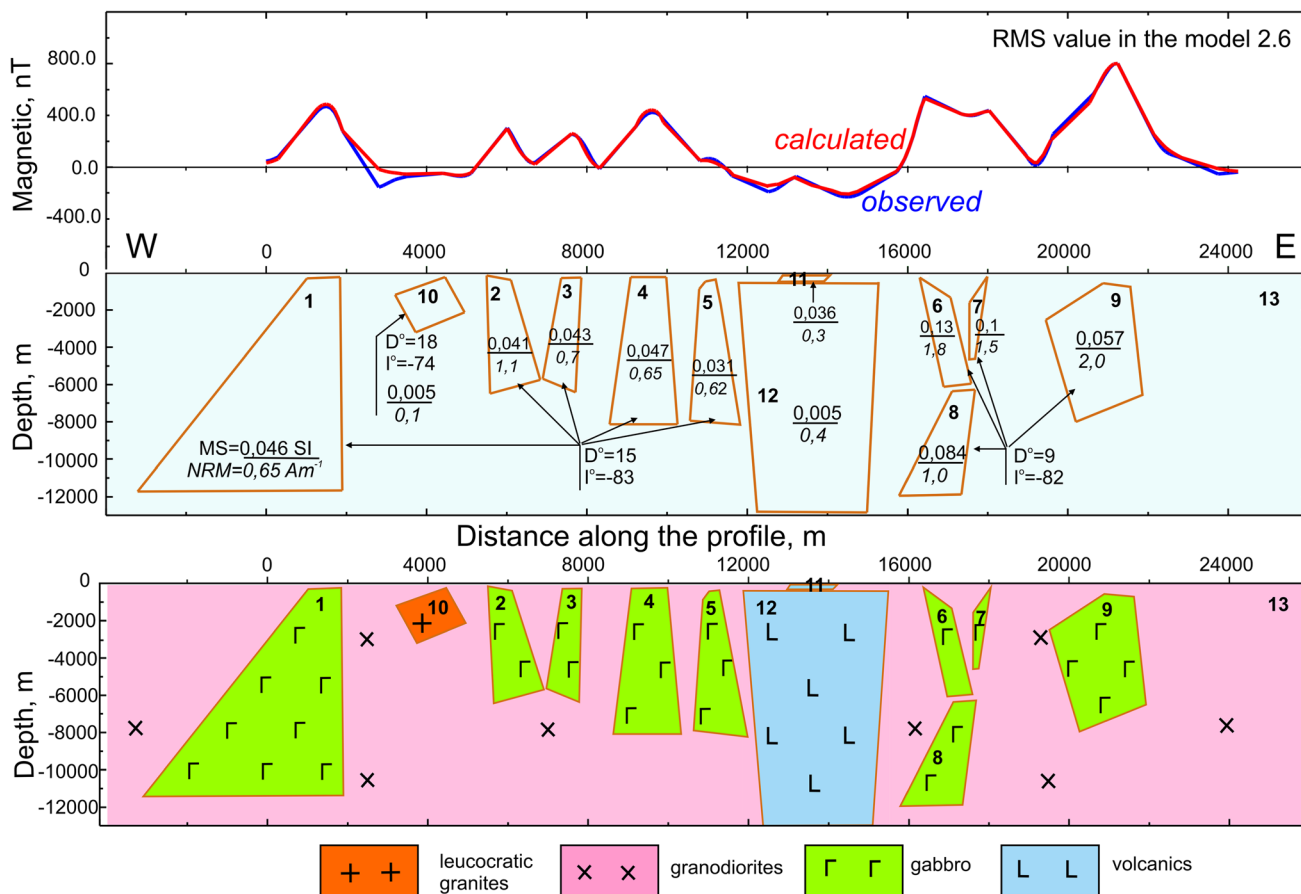
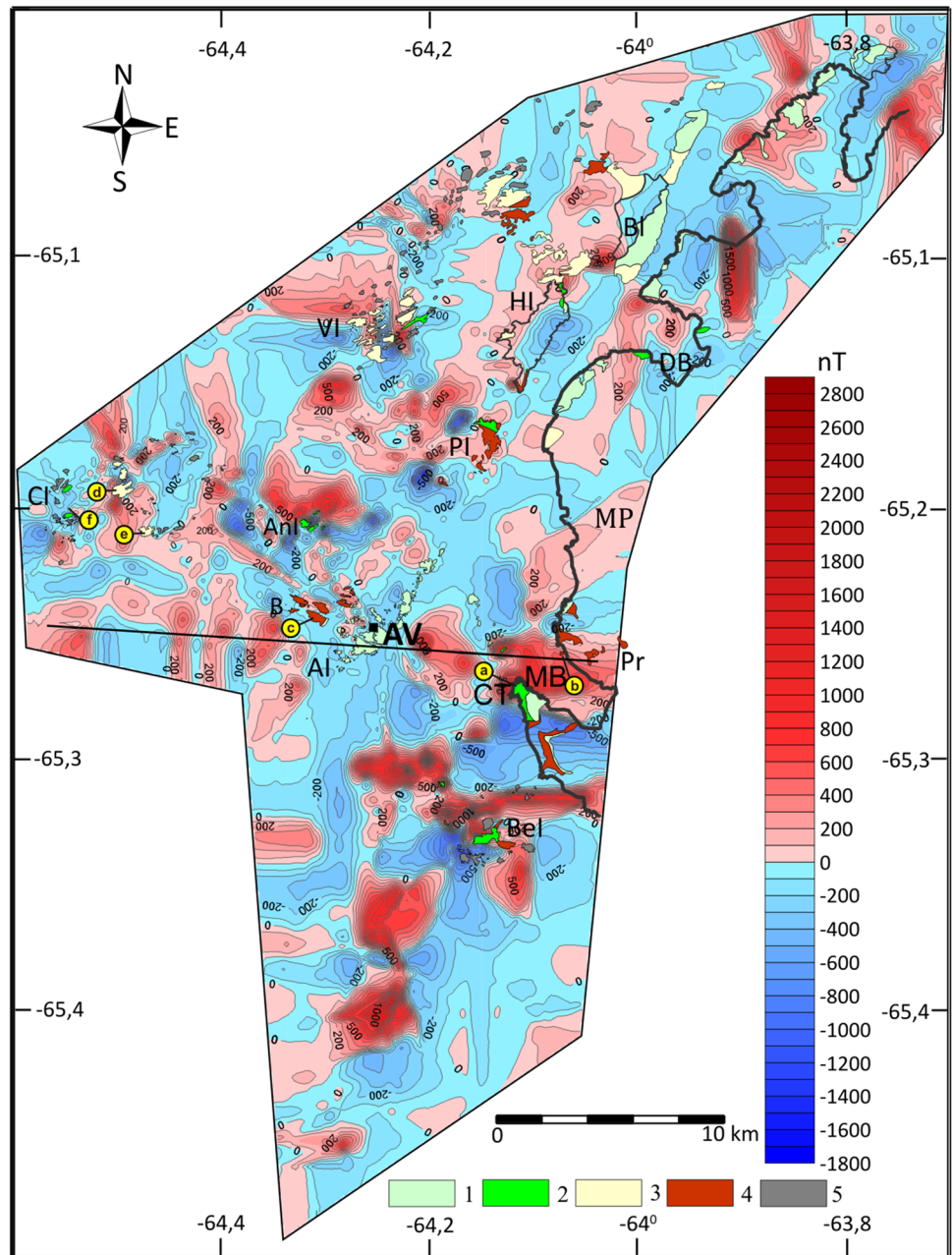


**Fig. 8** Magnetic model of the upper crust on the Pr1 profile (upper panel) and its geological interpretation (lower panel). The location of the profile is shown in Figs. 6, 7, 8. The magnetic model is represented by a set of bodies with magnetic parameters (Table 2): magnetic susceptibility MS (value above the line) in SI units, natural remanent magnetization NRM (value in italics below the line) in Am<sup>-1</sup>, NRM directions—declination (D°) and inclination (I°) in degrees

**Table 2** Magnetic parameters obtained from magnetic modeling on the Pr1 profile (Fig. 8, where the number of bodies corresponds to that in the table) and the directions of the vector of natural remanent magnetization (declination and inclination) in rocks of the study area. The D° and I° values are taken from (Bakhmutov and Shpyra 2011)

No	Rock types	Magnetic susceptibility (MS), SI	Natural remanent magnetization (NRM), Am <sup>-1</sup>	NRM directions	
				Declination D°	Inclination I°
1	Gabbro	0.046	0.65	15	-83
2	Gabbro	0.041	1.1	15	-83
3	Gabbro	0.043	0.7	15	-83
4	Gabbro	0.047	0.65	15	-83
5	Gabbro	0.031	0.62	15	-83
6	Gabbro	0.13	1.8	9	-82
7	Gabbro	0.1	1.5	9	-82
8	Gabbro	0.084	1.0	9	-82
9	Gabbro	0.057	2.0	9	-82
10	Leucocratic granite	0.005	0.1	18	-74
11	Volcanic rocks	0.036	0.3		
12	Volcanic rocks	0.005	0.4		
13	Granodiorites	0.02			

**Fig. 9** Local component of the anomalous magnetic field of the studied area with the locations of the outcrops from the geological map of Wilhelm Archipelago (Fig. 2; Mytrokhyn and Bakmutov 2021). For the explanations of symbols see Fig. 5. Legend: 1–Jurassic–Cretaceous volcanics of Kyiv Peninsula formation and Argentine islands formation; 2–gabbroid intrusions of mainly Early-Cretaceous age; 3–diorite intrusions of mainly early-cretaceous age; 4–granitoid intrusions of early-cretaceous, late-cretaceous and paleogene age; 5–unidentified rock outcrops

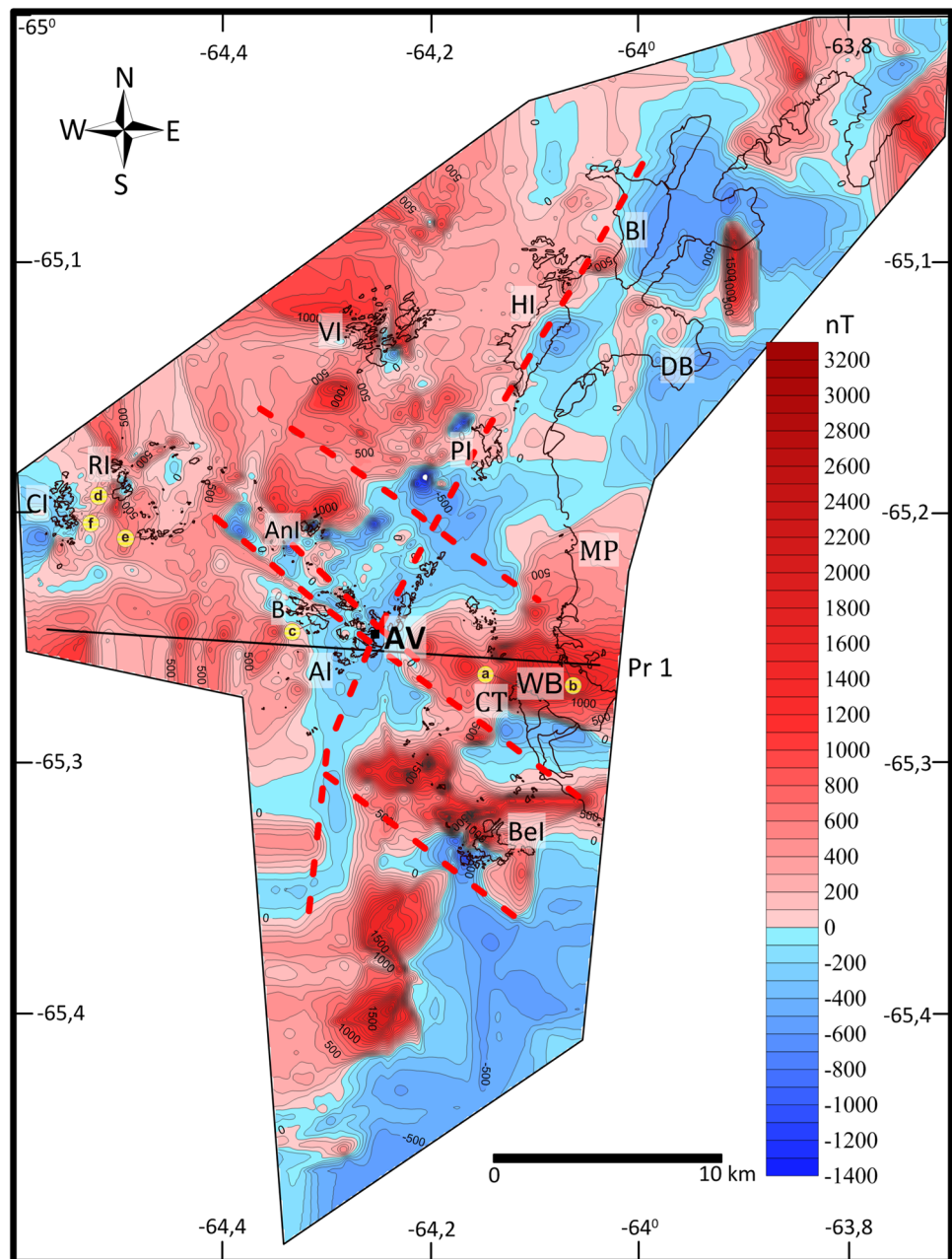


Jurassic–Lower Cretaceous age, gabbroid intrusive complexes of Cretaceous age (gabbro–norites, gabbro, stratified gabbro, gabbro–anorthosites), granitoid intrusive complexes represented by diorites, granodiorites and granite intrusions of Cretaceous to Paleogene age, and many dykes of differing ages and compositions. Since the composition of rocks is known only where ice-free outcrops exist on islands and the AP coast, the map of the magnetic field anomalies is essential for tracing the areal distribution, size, and interrelations of magmatic bodies.

- (2) Major and minor features were interpreted from the magnetic field map taking into account field observations and laboratory data on rock composition and magnetic properties. Distinct types of morphology and polarity were determined and assigned to recognized rock complexes. The oldest volcanic rocks of the Jurassic–Lower Cretaceous age can be recognized in two bands of the negative magnetic field around the Petermann and Argentine Islands, which trend N–NE, parallel to the AP coastline.
- (3) The largest distinct body, with a positive magnetic anomaly, is the Late Cretaceous–Lower Paleogene



**Fig. 10** Anomalous magnetic field of the Wilhelm Archipelago shelf zone with the identified fault system (thick dashed red lines). For explanations of the symbols see Fig. 5



granodiorite AP complex, which comprises diorites, granodiorites, and granites of varied compositions. Against a background magnetic field characteristic of granitoids, there are many more minor discrete magnetic anomalies above the bodies of Cretaceous gabbroids, along with local minima caused by granites depleted of ferromagnetic minerals.

- (4) Two-dimensional magnetic modeling shows the distribution of magnetic sources in the upper crust as a set of prisms with upper edges at hundreds of meters, and lower edges at 4–12 km depth. The magnetic susceptibilities of source rocks are in the range of 0.005–0.13 SI. Strong magnetic anomalies of 500–850 nT are

caused by gabbroid bodies against a background of weakly magnetic granitoids and volcanites.

- (5) The magnetic field pattern of the Wilhelm Archipelago in the Penola Strait area indicates the presence of sub-orthogonal tectonic faults. This includes a major NE-trending fault along the Penola Strait, and four younger NW-trending transform faults that cross the NE Penola fault. This fault system could be associated with different stages of continental margin evolution in the AP.

**Supplementary Information** The online version contains supplementary material available at <https://doi.org/10.1007/s11600-023-01190-6>.

**Acknowledgements** We gratefully acknowledge the State Institution National Antarctic Scientific Center of Ministry of Education and Sciences of Ukraine for support of our research in West Antarctica in the framework of the State Special-Purpose Research Program in Antarctica. Special thanks to members of wintering teams of “Akademik Vernadsky” base which provided the logistic support for field work during the expeditions. The authors are thankful to three anonymous reviewers for their valuable suggestions and comments which greatly improved the quality of the manuscript. This manuscript was prepared with the support of the National Science Center, Poland, research project no. UMO-2022/01/3/ST10/00033 (V. Bakhmutov).

**Author contributions** VB drafted the work and organized this study, put forward the main idea, assembled the geological-geophysical and rock magnetic parts of manuscript. TY made drafts of the ms, performed magnetic mapping, modeling and geological interpretation. MB performed magnetic mapping and 2D modeling OM described the geological setting. VS carried out all experiments for magnetic properties of rock. MO and VM designed the methodology and made contributions to the conception. VT, YN and AR contributed to the design and methodology of this study and together with YB, OR, YO, DL provided the magnetic survey with data acquisition and analysis.

## Declarations

**Conflict of interest** On behalf of all authors, the corresponding author states that there is no conflict of interest.

**Ethical approval** This paper complies with the ethical standards of research and methodology.

**Open Access** This article is licensed under a Creative Commons Attribution 4.0 International License, which permits use, sharing, adaptation, distribution and reproduction in any medium or format, as long as you give appropriate credit to the original author(s) and the source, provide a link to the Creative Commons licence, and indicate if changes were made. The images or other third party material in this article are included in the article’s Creative Commons licence, unless indicated otherwise in a credit line to the material. If material is not included in the article’s Creative Commons licence and your intended use is not permitted by statutory regulation or exceeds the permitted use, you will need to obtain permission directly from the copyright holder. To view a copy of this licence, visit <http://creativecommons.org/licenses/by/4.0/>.

## References

- Artemenko G, Bakhmutov V, Samborskaya I, Bakhmutova L (2013) Magma layering of gabbroids of Antarctic Peninsula batholith. *Ukr Antarct J* 12:30–33. <https://doi.org/10.33275/1727-7485.12.2013.242>
- Bakhmutov V, Shpyra V (2011) Palaeomagnetism of late cretaceous–paleocene igneous rocks from the western part of Antarctic Peninsula (Argentine islands Archipelago). *Geol Q* 55(4):285–300
- Bakhmutov VG, Gladkochub DP, Shpyra VV (2013) Age position, geodynamic specifics and paleomagnetism of intrusive complexes of the western coast of the Antarctic Peninsula. *Geophys J* 35(3):3–30. <https://doi.org/10.24028/gzh.0203-3100.v35i3.2013.116387>
- Birkenmajer K (1994) Evolution of the Pacific margin of the northern Antarctic Peninsula: an overview. *Geol Rundsch* 83(2):309–321. <https://doi.org/10.1007/BF00210547>
- Blakely RJ, Brocher TM, Wells RE (2005) Subduction-zone magnetic anomalies and implications for hydrated forearc mantle. *Geology* 33(6):445–448. <https://doi.org/10.1130/G21447.1>
- Burton-Johnson A, Riley TR (2015) Autochthonous versus accreted terrane development of continental margins: a revised in situ tectonic history of the Antarctic Peninsula. *J Geol Soc* 172(6):822–835. <https://doi.org/10.1144/jgs2014-110>
- Catalán M, Galindo-Zaldivar J, Martín Davila JM, Martos YM, Maldonado A, Gambôa L, Schreider A (2013) Initial stages of oceanic spreading in the bransfield rift from magnetic and gravity data analysis. *Tectonophysics* 585:102–112. <https://doi.org/10.1016/j.tecto.2012.09.016>
- Clark DA (1997) Magnetic petrophysics and magnetic petrology: aids to geological interpretation of magnetic surveys. *AGSO J Aust Geol Geophys* 17(2):83–103
- Clowes RM, Hyndman RD (2002) Geophysical studies of the northern Cascadia subduction zone off western Canada and their implications for great earthquake seismotectonics: a review. In: Fujinawa Y, Yoshida A (eds) *Seismotectonics in Convergent Plate Boundary*. Terra Scientific Publishing Company, Tokyo, pp 1–23
- Curtis R (1966) The petrology of the Graham coast Graham land British Antarctic survey. *Sci Rep* 50:51
- Elliot DH (1964) The petrology of the Argentine islands. *British Antarctic Survey Science Report*, Cambridge
- Ferraccioli F, Jones PC, Vaughan APM, Leat PT (2006) New aerogeophysical view of the Antarctic Peninsula: more pieces, less puzzle. *Geophys Res Lett*. <https://doi.org/10.1029/2005GL024636>
- Ferraccioli F, von Frese R, Ghidella M, Thybo H (2013) Recent advances in Antarctic geomagnetism and lithospheric studies. *Tectonophysics*. [https://doi.org/10.1016/S0040-1951\(13\)00038-3](https://doi.org/10.1016/S0040-1951(13)00038-3)
- Frost BR (1991) Magnetic petrology: factors that control the occurrence of magnetite in crustal rocks. *Rev Mineral Geochem* 25(1):489–509
- Garrett SW (1990) Interpretation of reconnaissance gravity and aeromagnetic surveys of the Antarctic Peninsula. *J Geophys Res* B5:6759–6777. <https://doi.org/10.1029/JB095iB05p06759>
- Ghidella ME, Forsberg R, Greenbaum JS, Olesen AV, Zakrajsek AF, Blankenship DD (2011) Magnetic anomaly data from a regional survey: from Tierra del Fuego to northern Palmer land. *Antarct Penins Latinmag Lett* 1(A19):1–7
- Golynsky AV, Masolov VN (2000) Interpretation of ground and aeromagnetic surveys of Palmer land. *Antarct Penins Ann Geophys* 42(2):333–351. <https://doi.org/10.4401/ag-3649>
- Golynsky A, Chiappini M, Damaske D, Ferraccioli F, Ferris J, Finn C, Ghidella M, Ishihara T, Johnson A, Kim HR, Kovacs L, LaBrecque J, Masolov V, Nogi Y, Purucker M, Taylor P, Torta M (2001) ADMAP–magnetic anomaly map of the Antarctic, 1:10 000 000 scale map. *BAS (misc)* 10:1109–1112
- Golynsky A, Bell R, Blankenship D, Damaske D, Ferraccioli F, Finn C, Golynsky D, Ivanov S, Jokat W, Masolov V, Riedel S, von Frese R, Young D, ADMAP Working Group (2013) Air and shipborne magnetic surveys of the Antarctic into the 21st century. *Tectonophysics* 585:3–12. <https://doi.org/10.1016/j.tecto.2012.02.017>
- Golynsky AV, Golynsky DA, Ferraccioli F, Hong JK et al (2018) ADMAP 2: Magnetic anomaly map of the Antarctic, 1:10 000 000, KOPRI map series 1, Incheon. *Korea Polar Res Ins*. <https://doi.org/10.22663/ADMAP.V2>
- Grad M, Guterch A, Janik T, Środa P (2002) Seismic characteristic of the crust in the transition zone from pacific ocean to the northern Antarctic Peninsula, west Antarctica. *R Soc N Z Bull* 35:493–498
- Grunow A (1993) New paleomagnetic data from Antarctic Peninsula and their tectonic implication. *J Geophys Res* 98(B8):13815–13833. <https://doi.org/10.1029/93JB01089>

- Janik T (1997) Seismic crustal structure of the bransfield strait, west Antarctica. *Pol Polar Res* 18:171–225
- Janik T, Środa P, Grad M, Guterch A (2006) Moho depths along the Antarctic Peninsula and crustal structure across the landward projection of the hero fracture zone. In: Fütterer DK, Damaske D, Kleinschmidt G, Miller H, Tessensohn F (eds) *Antarctica: contributions to global earth sciences*. Springer, New York, pp 229–236. [https://doi.org/10.1007/3-540-32934-X\\_27](https://doi.org/10.1007/3-540-32934-X_27)
- Janik T, Grad M, Guterch A, Środa P (2014) The deep seismic structure of the earth's crust along the Antarctic Peninsula—a summary of the results from polish geodynamical expeditions. *Glob Planet Change* 123:213–222. <https://doi.org/10.1016/j.gloplacha.2014.08.018>
- Johnson AC (1999) Interpretation of new aeromagnetic anomaly data from central Antarctic Peninsula. *J Geophys Res* 104(B3):5031–5046. <https://doi.org/10.1029/1998JB900073>
- Jordan TA, Neale RF, Leat PT, Vaughan APM, Flowerdew MJ, Riley TR, Whitehouse MJ, Ferraccioli F (2014) Structure and evolution of Cenozoic arc magmatism on the Antarctic Peninsula: a high resolution aeromagnetic perspective. *Geophys J Int* 198(3):1758–1774. <https://doi.org/10.1093/gji/ggu233>
- Jordan TA, Riley TR, Siddoway CS (2020) The geological history and evolution of west Antarctica. *Nat Rev Earth Environ* 1:117–133. <https://doi.org/10.1038/s43017-019-0013-6>
- Kim HR, von Frese RRB, Golynsky AV, Taylor PT, Kim JW (2004) Applications of satellite magnetic observations for estimating near-surface magnetic anomalies. *Earth, Planets Space* 56:955–966. <https://doi.org/10.1186/BF03351793>
- Kim HR, von Frese RRB, Golynsky AV, Gaya-Pigue LR, Ferraccioli F (2007) Improved magnetic anomalies of the Antarctic lithosphere. *Geophys J Int* 171(1):119–126. <https://doi.org/10.1111/j.1365-246X.2007.03516.x>
- Kovalenko-Zavoytskiy VM, Ivashenko IM (2006) Mathematical provision for interpretation of  $\Delta B_a$  field of regional magnetic anomalies. *Geophys J* 5(28):18–30
- Larter RD, Barker PF (1991) Effects of ridge crest trench interaction on Antarctic-phoenix spreading: forces on a young subducting plate. *J Geophys Res* 96(B12):19583–19607. <https://doi.org/10.1029/91JB02053>
- Larter RD, Cunningham AP, Barker PF, Gohl K, Nitsche FP (2002) Tectonic evolution of the Pacific margin of Antarctica 1. Late Cretaceous tectonic reconstructions. *J Geophys Res* 107(B12):EPM5–EPM19. <https://doi.org/10.1029/2000JB000052>
- Leat PT, Scarrow JH, Millar IL (1995) On the Antarctic Peninsula batholith. *Geol Mag* 132(4):399–412. <https://doi.org/10.1017/S0016756800021464>
- Maksymchuk VYu, Bakhmutov VG, Horodyskiy YuM, Chobotok IO (2009) Results and perspectives of tectonomagnetic investigations in the western Antarctic. *Ann Geophys* 52(1):35–43. <https://doi.org/10.4401/ag-4571>
- Maslanyj MP, Garrett SW, Johnson AC, Renner RGB, Smith AM (1991) Aeromagnetic anomaly map of West Antarctica, BAS GEOMAP Series Geophysics Map and Suppl Text. British Antarctic Survey, Cambridge
- Mytrokhyn O, Bakhmutov V (2019) Stratigraphy of the area of Ukrainian Antarctic akademik vernadsky station. *Ukr Antarc Journal* 18(1):45–61. [https://doi.org/10.33275/1727-7485.1\(18\).2019.12](https://doi.org/10.33275/1727-7485.1(18).2019.12)
- Mytrokhyn O, Bakhmutov V (2021) Geological mapping of the Ukrainian Antarctic station area (Wilhelm Archipelago and Kyiv Peninsula, Graham Coast). In: Proceedings of the XV international scientific conferencemonitoring of geological processes and ecological condition of the environment, 17–19 Nov 2021, Kyiv, Ukraine. <https://doi.org/10.3997/2214-4609.20215K2082>
- Mytrokhyn O, Bakhmutov V, Aleksieienko A, Mytrokhina T, Marushchenko O (2021) Intrusive-magmatic complexes of Wilhelm Archipelago, west Antarctica (part 1—intrusions of gabbroids, diorites and granitoids). *Geology* 95(4):6–15. <https://doi.org/10.17721/1728-2713.95.01>
- Mytrokhyn O, Bakhmutov V, Gavryliv L (2022) Intrusive magmatic complexes of Wilhelm Archipelago, west Antarctica (part 2—hypabyssal and subvolcanic dyke rocks). *Geology* 98(3):5–14. <https://doi.org/10.17721/1728-2713.98.01>
- Orlyuk MI, Romenets AA (2009) Spatio-temporal structure of the geomagnetic field in the area of the Argentine islands archipelago (AV station). In: Proceedings of the IX international science conference monitoring of geological processes, 14–17 Oct 2009, Kyiv, Ukraine, p 92–94 (in Russian)
- Pankhurst RJ (1983) Rb-Sr constraints on the ages of basement rocks of the Antarctic Peninsula. In: Oliver RL, James PR, Jago JB (eds) *Antarctic earth science*. Cambridge University Press, Cambridge, pp 367–371
- Pankhurst RJ, Riley TR, Fanning CM, Kelley SP (2000) Episodic silicic volcanism in Patagonia and the Antarctic Peninsula: chronology of magmatism associated with the break-up of Gondwana. *J Petrol* 41(5):605–625. <https://doi.org/10.1093/ptetrology/41.5.605>
- Pelayo AM, Wiens DA (1989) Seismotectonics and relative plate motions in the Scotia sea region. *J Geophys Res* 94(B6):7293–7320. <https://doi.org/10.1029/JB094iB06p07293>
- Poblete F, Arriagada C, Roperch P, Astudillo N, Hervé F, Kraus S, Le Rouxm JP (2011) Paleomagnetism and tectonics of the south Shetland islands and the northern Antarctic Peninsula. *Earth Planet Sci Lett* 302(3–4):299–313. <https://doi.org/10.1016/j.epsl.2010.12.019>
- Renner RGB, Dijkstra BJ, Martin JL (1982) Aeromagnetic surveys over the Antarctic Peninsula. In: Craddock C (ed) *Antarctic geoscience*. University of Wisconsin Press, Madison, pp 363–367
- Renner RGB, Sturgeon LJS, Garrett SW (1985) Reconnaissance gravity and aeromagnetic surveys of the Antarctic Peninsula. *British Antarctic Survey Science Report*, Cambridge
- Riley TR, Leat PT, Pankhurst RJ, Harris C (2001) Origins of large volume rhyolitic volcanism in the Antarctic Peninsular and Patagonia by crustal melting. *J Petrol* 42(6):1043–1065. <https://doi.org/10.1093/ptetrology/42.6.1043>
- Riley TR, Flowerdew MJ, Pankhurst RJ, Curtis ML, Millar IL, Fanning CM, Whitehouse MJ (2017) Early Jurassic magmatism on the Antarctic Peninsula and potential correlation with the subcordilleran plutonic belt of Patagonia. *J Geol Soc* 174(2):365–376. <https://doi.org/10.1144/jgs2016-053>
- Stacey D, Robertson M, Wiens DA, Shore PJ, Vera E, Dorman LM (2003) Seismicity and tectonics of the south Shetland Islands and bransfield strait from a regional broadband seismograph deployment. *J Geophys Res*. <https://doi.org/10.1029/2003JB002416>
- Saltus RW, Hudson TL, Connard GG (1999) A new magnetic view of Alaska. *GSA Today* 9(3):1–6
- Shpyra V, Bakhmutov V, Bakhmutova L, Gladkochub D, Koshelev A, Skarboviychuk T, Yakukhno V (2014) Magnetic and density characteristics of igneous rocks near the Ukrainian antarctic station akademik vernadsky. *Ukr Antarc J* 13:81–93. <https://doi.org/10.33275/1727-7485.13.2014.215>
- Soloviev VD, Bakhmutov VG, Korchagin IN, Yegorova TP (2018) New geophysical data about the Pacific margin (west Antarctica) magnetic anomaly sources and origin. *Ukr Antarc J* 1(17):20–31. [https://doi.org/10.33275/1727-7485.1\(17\).2018.28](https://doi.org/10.33275/1727-7485.1(17).2018.28)
- Środa PM, Grad A, Guterch A (1997) Seismic models of the earth's crustal structure between the south pacific and the Antarctic Peninsula. In: Ricci CA (ed) *The Antarctic region: geological evolution and processes*. Terra Antarctica Publication, Siena, pp 685–689

- Storey BC, Garrett SW (1985) Crustal growth of the Antarctic Peninsula by accretion, magmatism and extension. *Geol Mag* 122(1):5–14. <https://doi.org/10.1017/S0016756800034038>
- Tangeman JA, Mukasa SB, Grunow AM (1996) Zircon U-Pb geochronology of plutonic rocks from the Antarctic Peninsula: confirmation of the presence of unexposed paleozoic crust. *Tectonics* 15(6):1309–1324. <https://doi.org/10.1029/96TC00840>
- Thompson MRA, Pankhurst RJ (1983) Age of post-gondwanian calc-alkaline volcanism in the Antarctic Peninsula region. In: Oliver RL, James PR, Jago JB (eds) *Antarctic Earth Science*. Cambridge University Press, Cambridge, pp 328–333
- Vaughan APM, Storey BC (2000) The Eastern Palmer land shear zone: a new terrane accretion model for the mesozoic development of the Antarctic Peninsula. *J Geol Soc Lond* 157(6):1243–1256. <https://doi.org/10.1144/jgs.157.6.1243>
- Vaughan APM, Pankhurst R (2008) Tectonic overview of the west Gondwana margin. *Gondwana Res* 13(2):150–162. <https://doi.org/10.1016/j.gr.2007.07.004>
- Vaughan APM, Eagles G, Flowerdew MJ (2012) Evidence for a two-phase Palmer land event from crosscutting structural relationships and emplacement timing of the lassiter goast intrusive suite, Antarctic Peninsula: implications for mid-cretaceous southern ocean plate configuration. *Tectonics*. <https://doi.org/10.1029/2011TC003006>
- von Frese RRB, Taylor PT, Chiappini M (2002) Magnetic anomalies of the Antarctic. *Tectonophysics*. [https://doi.org/10.1016/S0040-1951\(01\)00233-5](https://doi.org/10.1016/S0040-1951(01)00233-5)
- Wendt AS, Vaughan APM, Ferraccioli F, Grunow AM (2013) Magnetic susceptibilities of rocks of the Antarctic Peninsula: implications for the redox state of the batholith and the extent of metamorphic zones. *Tectonophysics* 585:48–67. <https://doi.org/10.1016/j.tecto.2012.07.011>
- Yegorova T, Bakhmutov V (2013) Crustal structure of the Antarctic Peninsula sector of the Gondwana margin around Anvers island from geophysical data. *Tectonophysics* 585:77–89. <https://doi.org/10.1016/j.tecto.2012.09.029>
- Yegorova T, Bakhmutov V, Janik T, Grad M (2011) Joint geophysical and petrological models for the lithosphere structure of the Antarctic Peninsula continental margin. *Geophys J Int* 184:90–110. <https://doi.org/10.1111/j.1365-246X.2010.04867.x>
- Yegorova T, Gobarenko V, Murovskaya A (2022) Jurassic-Cretaceous magmatic arcs in the eastern black sea: evidence from geophysical studies and 2D modeling. *J Geodyn*. <https://doi.org/10.1016/j.jog.2021.101890>
- Zavoyskiy VM (1978) Calculation of magnetic fields from anisotropic three-dimensional bodies in problems of magnetic prospecting. *Phys Earth* 1:76–85 (**in Russian**)
- Zheng GG, Liu X, Liu S, Zhang SH, Zhao Y (2018) Late mesozoic–early cenozoic intermediate-acid intrusive rocks from the Gerlache Strait area, Antarctic Peninsula: zircon U–Pb geochronology, petrogenesis and tectonic implications. *Lithos* 312–313:204–222. <https://doi.org/10.1016/j.lithos.2018.05.008>